Thin-Film Behavior of Poly(methyl methacrylates). 1. Monolayers at the Air–Water Interface

R. H. G. Brinkhuis and A. J. Schouten*

Department of Polymer Chemistry, University of Groningen, Nijenborgh 16, 9747 AG Groningen, The Netherlands

Received June 22, 1990; Revised Manuscript Received September 6, 1990

ABSTRACT: The monolayer behavior of PMMA of varying tacticities at the air–water interface was studied. A difference in lateral cohesive energy is argued to be responsible for the fact that the pressure area isotherms of isotactic PMMA deviate strongly from those of syndiotactic PMMA. At low surface pressures the isotactic PMMA monolayer can be characterized as an expanded type monolayer, whereas syndiotactic PMMA forms a condensed type monolayer. At areas of about 20 Å^2/monomeric unit a transition can be observed in the pressure–area isotherm of isotactic PMMA. This transition was studied as a function of molecular weight, temperature, and compression speed. From the results it is deduced that the transition corresponds to a two-dimensional pseudocrystallization process in which the isotactic PMMA assumes a double-helix conformation in the monolayer, similar to the three-dimensional crystal structure. From an Avrami analysis it is inferred that the kinetics of this crystallization can be described by an activated nucleation, followed by a one-dimensional growth.

Introduction

Langmuir–Blodgett films of polymers have been the subject of extensive research during the past decades,[1-3] but the research efforts have increased drastically in the past decade because of possible applications in nonlinear optical devices and other fields such as biosensors and microlithography. For these applications, use can be made of the well-defined film deposition and the orientational characteristics of polymeric Langmuir–Blodgett films.

A great deal of attention has been focused on comblike polymers with large hydrophobic side chains (polymeric analogues of low molecular weight amphiphilic molecules),[4-11] but also "linear" polymers with short side chains have been studied extensively. Studies of poly(methyl methacrylate), as a "standard" polymer, have been reported by numerous authors.[2,12-30] The monolayer properties and behavior were studied by pressure–area isotherms,[2,12,13,24] dipole measurements,[2] ellipsometry,[18] surface light scattering,[26] atomic force microscopy,[27,28] and fluorescence spectroscopy.[25]

Crisp[1,2] was the first author to systematically discuss monolayer properties of polymeric substances, especially of polyacrylates and polymethacrylates. He reported that PMMA forms patchy structures, consisting of condensed islands of PMMA at low surface coverages. He also proposed conformations for the ester groups in these materials at the water–air interface, based on measurements of the dipole moments. Since then a lot of information has been published about PMMA monolayers at the water surface, such as the behavior of its copolymers,[22] its monolayer miscibility with low molecular weight substances and other polymers, the stability and hysteresis phenomena that may occur,[17,21,22,29,30] mechanical properties,[17,21,24,30] and the film thickness.[18,26] The conformation of the PMMA at the air–water interface has not been exactly elucidated though.

With all this work on PMMA, the matter of the tacticity of the polymers has hardly been addressed. Beredjick and Ries[12-14] published isotherms of isotactic, syndiotactic, atactic, and stereoblock PMMA almost 30 years ago: the pressure–area isotherms of the isotactic (and of the stereoblock type) polymer proved to be quite different from those of syndiotactic and atactic samples. No adequate explanation was given at that time. Sutherland and Miller[15] also reported an isotherm for isotactic poly(methyl methacrylate), but since then monolayers of isotactic PMMA have not received much attention in the literature.

Sutherland and Miller[15] also reported isotherms of several polymeric *tert*-butyl esters of varying tacticity and explained the observed differences by a different packing efficiency of the segments in the monolayer for different tacticities.

Stroeve[17] has suggested differences in tacticity between his syndiotactic PMMA and Gabriellis atactic PMMA to explain some differences observed in their respective Π–A isotherms; no values for the tacticity were reported though.

Anticipating using transferred Langmuir–Blodgett layers to prepare model thin films and model surfaces (e.g., for surface analysis techniques), we started studying the thin-film behavior of poly(methyl methacrylates). The aim of the work presented in this article is to examine the effects of stereoregularity on monolayer and thin-film behavior in more detail and to focus on the anomalous monolayer behavior of isotactic PMMA.

Experimental Section

Materials. Highly isotactic PMMA (samples 1–16) was synthesized in toluene solution either at room temperature with C_6H_5MgBr as initiator[31] or at −80 °C with *t*-BuMgBr as initiator, according to the procedure described by Hatada.[32] In both cases triad tacticities of more than 96% iso were obtained, with only in the case of the first synthesis route some small deviations for the lowest molecular weight fractions.

Moderately isotactic PMMA samples were obtained by anionic polymerization in toluene with *t*-BuLi as initiator at varying temperatures (−55 °C for samples 18–20 and −25 °C for samples 21 and 22) or with *n*-BuLi as initiator at −70 °C (sample 17).

Moderately syndiotactic PMMA (sample 24, "atactic") was synthesized by an ordinary radical polymerization using AIBN as initiator in a 50 v/v % toluene solution at 70 °C. The syndiotactic PMMA used in this study was synthesized by a Ziegler–Natta type polymerization (sample 25).[33]

Some of the isotactic samples studied were selectively deuterated. We have no indication whatsoever that the deuteration affected the physical behavior of the polymers in any way relevant to the results reported here. The triad tacticity of the α-CD_3 PMMA ($(CH_2C(CD_3)(CO_2CH_3))_n$) could not be determined directly from the ^{1}H NMR spectrum but is assumed to be similar to that of other polymer samples prepared according to the same procedure;[32] no racemic diads could be observed in the ^{1}H NMR spectrum.

Table I

sample	$10^{-3}\bar{M}_n$	D	triad tacticity i	h	s	remarks
1	770	1.5	97	3	0	
2	250	1.10	97	3	0	
3	95	1.20	97	3	0	
4	54	1.19	97	3	0	
5	36	1.16	97	3	0	
6	24	1.21	97	3	0	
7	21	1.16	97	3	0	
8	19	1.17	97	3	0	
9	18.9	1.14	97	3	0	$CH_2C(CH_3)(CO_2CD_3)$
10	13.3	1.19	97	3	0	
11	11.1	1.22	(97	3	0)	$CH_2C(CD_3)(CO_2CH_3)$
12	8.4	1.15	97	3	0	$CD_2C(CH_3)(CO_2CH_3)$
13	7.8	1.23	94	5	1	
14	5.3	1.38	92	6	2	
15	4.0	1.20	90	7	3	
16	2.8	1.35	89	8	3	
17	29	1.25	91	7	2	
18	28	1.16	80	16	4	
19	17.7	1.13	81	15	4	
20	68	1.33	83	14	3	
21	28	1.21	67	27	6	
22	78	1.13	67	26	7	
24	43	1.16	3	34	63	
25	25	1.09	1	14	85	

If necessary, polymers were fractionated to a narrow molecular weight distribution by precipitation from critical acetone/water solvent mixtures.

Triad tacticities were determined with a 300-MHz Varian VXR 300 NMR instrument, and molecular weight distributions were measured with a Waters 150-C GPC equipped with Styragel columns, using monodisperse polystyrene standards. Triad tacticities and the molecular weight characteristics are listed in Table I.

Monolayers. Monolayer properties were studied by using a computer-controlled Lauda Filmbalance FW2. The surface pressure could be measured with an accuracy of about 0.05 mN/m. The subphase was water, purified by double distillation and subsequent filtration through a Milli-Q purification system. No significant surface pressure was measured before spreading of the polymer solution upon compressing the area to 2.5% of its initial value.

Polymers were spread from chloroform solutions (Uvasol quality, concentrations 0.3–0.5 g/L). Temperature and compression speed were varied. For the Π–A isotherms compression was started at a standard area of 60 Å^2/molecular unit, 5 min after spreading, to allow the solvent to evaporate and the monolayer to fill the available area completely.

Results and Discussion

Figure 1 shows the pressure–area isotherms of syndiotactic, atactic, and isotactic PMMA. It can easily be seen that the isotactic material has a distinctly different monolayer behavior as compared to the atactic and the syndiotactic PMMA samples. In this article we will focus on the behavior of isotactic PMMA at the air–water interface, which has been studied to only a very limited extent so far. The only authors to report pressure–area isotherms of isotactic PMMA were Beredjick[12-14] and Sutherland and Miller.[15] Beredjick interpreted the Π–A isotherms as consisting of at least three distinct parts (0–8 mN/m, 8 to ~18 mN/m, and the region at higher surface pressures) and calculated characteristic areas for these regions by extrapolation to zero pressure. The structural nature of the deviating monolayer behavior of isotactic PMMA was not studied in detail though.

The linear extrapolation of the low-pressure part of the isotherm is quite arbitrary, since there is no actually linear part in the isotherm at these pressures. Instead, this region is very much similar to pressure–area isotherms of expanded type polymeric monolayers as poly(vinyl acetate)

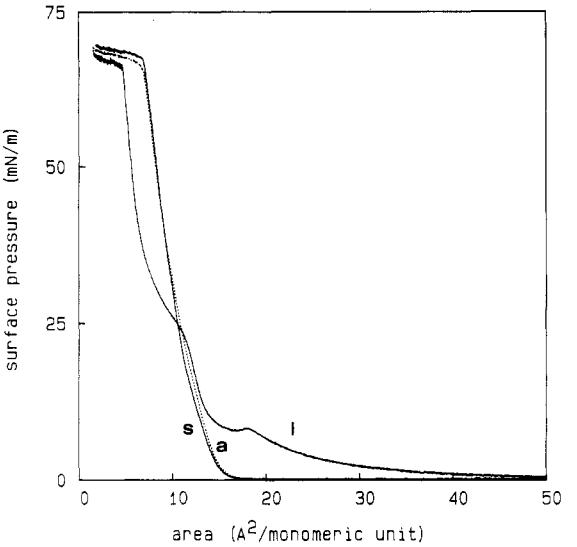

Figure 1. Pressure–area isotherms of isotactic (sample 5, i), "atactic" (sample 24, a, dotted line) and syndiotactic (sample 25, s, solid line) PMMA; temperature 22 °C, compression speed 2 Å^2/(monomeric unit min).

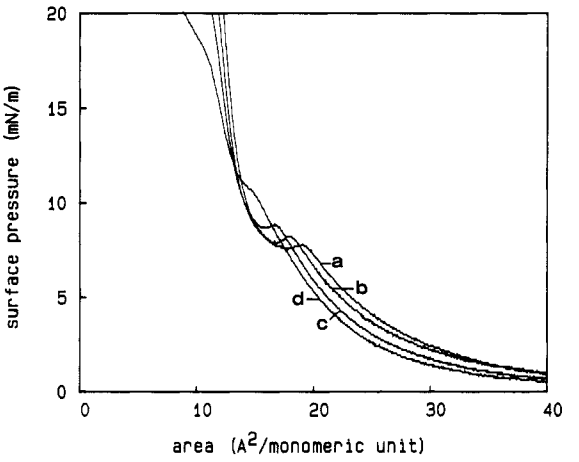

Figure 2. Pressure–area isotherms of isotactic PMMA (sample 5); compression speed 2 Å^2/(monomeric unit min), temperature (a) 10, (b) 22, (c) 32, (d) 41 °C.

and poly(methyl acrylate), where a surface pressure builds up even at large areas because of the geometric constraints (which limit the number of available configurations and thus the entropy) imposed on the two-dimensional polymeric coils at the air–water interface. Therefore the area obtained from the linear extrapolation of this part of the curve has no direct physical significance.

The "transition" observed at about 8 mN/m is characteristic for the isotherms of isotactic PMMA in contrast to the syndiotactic (or atactic) samples, which exhibit no such phenomenon at low surface pressures. The isotherm of isotactic PMMA also shows an inflection point at about 20 mN/m, but above this pressure the monolayers no longer become stable. We will focus on the behavior of the monolayers up to pressures of about 20 mN/m and the transition that can be observed at 8 mN/m in the isotherm of isotactic PMMA.

Figure 2 shows the isotherms of isotactic PMMA as a function of temperature. The low-pressure part of the isotherms reflecting the behavior of the monolayer in the expanded state exhibits a surprising temperature dependence: the surface pressure of the monolayer associated with a constant area per monomeric unit decreases with increasing temperature, opposite to what would be expected for an entropy-associated pressure (and opposite to, e.g., the behavior of poly(methyl acrylate).[34] This phenomenon is discussed later in this article.

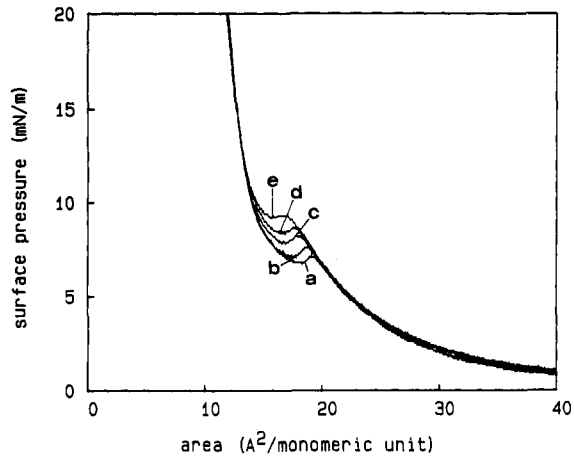

Figure 3. Pressure–area isotherms of isotactic PMMA (sample 5), temperature 22 °C, compression speed (a) 0.25, (b) 0.67, (c) 2.0, (d) 4.0, (e) 12.0 Å²/(monomeric unit min).

Another interesting observation in the pressure–area isotherms is the shift of the aforementioned transition upon raising the temperature; the transition pressure increases with increasing temperature, suggesting a negative entropy change to be associated with the transition process involved. Simultaneously, the specific area corresponding to the onset of the transition decreases with increasing temperature. At 50 °C the isotherms no longer exhibit any sign of the transition.

Remarkably strong is the effect of the compression rate on the shape of the pressure–area isotherms (Figure 3). As the compression rate is lowered, the pressure where the transition becomes evident drops significantly (from 9.2 mN/m at 12 Å²/(monomeric unit min) to 7.0 mN/m at 0.25 Å²/(monomeric unit min)). At the same time, a "dip" (a drop in the surface pressure as compression proceeds just past the onset of the transition) remains observable even at low compression rates (and even more clearly so!). The strong compression speed dependence clearly indicates that the monolayer transition is associated with a rather slow process. The "dip" observed in the isotherms is a more puzzling phenomenon. If a simple phase transition was to take place between two phases of equal thermodynamic potential, with a transformation speed dependent only on the surface pressure, one would anticipate the pressure to remain constant or to rise slowly during the transition. An interpretation of the actual shape of the isotherm in the transition region in terms of a "normal" overshoot mechanism cannot explain the fact that this pressure dip remains clearly observable even at very low compression speeds (down to 0.2 Å²/(monomeric unit min)). We will discuss these phenomena in more detail later on in this article.

Monolayers of isotactic PMMA become stable at 5 mN/m as well as at 12 mN/m, before and after the transition, respectively. The time required for the monolayer stabilization is about 30–40 min. The monolayers can be transferred to solid substrates as hydrophobized silicon, ZnS, or gold. Transfer ratios are listed in Table II.

Hysteresis. From hysteresis experiments we learn that the monolayer compression is perfectly reversible as long as the monolayer is compressed to an area corresponding to a point in the isotherm before the transition. When the monolayer is compressed to a point beyond the transition pressure (Figure 4), the decompression curve does not follow the compression curve: the pressure drops sharply at the beginning of the decompression and approaches the compression pressure–area isotherm only at large areas. No sign of the compression transition can be seen upon decompression, not even at very slow decompression rates. We conclude that for isotactic PMMA the monolayer compression is *not instantaneously* reversible beyond the transition point.

Table II
Typical Transfer Ratios

	5 mN/m		12 mN/m	
mol wt	down	up	down	up
low (<20 000)			0.2–0.3	1.0
intermediate	0–0.3	1.0	0.4	1.0
high (>200 000)[a]			0.4	1.0–0.6

[a] Transfer starts off similarly to intermediate MW, but upstroke transfer decreases with subsequent layers.

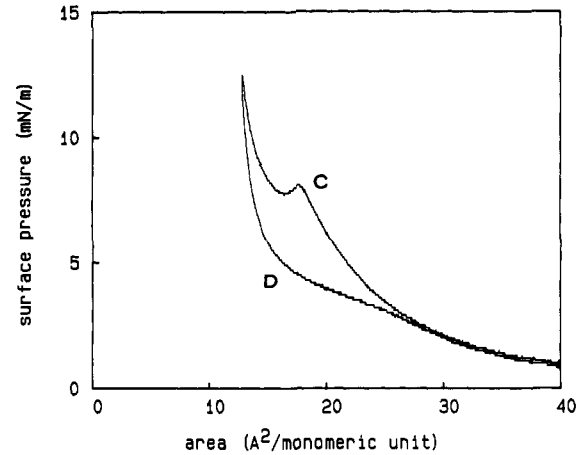

Figure 4. Hysteresis plot for sample 5, temperature 22 °C, compression speed 2 Å²/(monomeric unit min), pause time 1 min, maximum pressure set at 12 mN/m.

Upon recompressing the same monolayer however (starting from 60 Å²/monomeric unit), the surface pressure follows the same isotherm as the first compression run; evidently no eventually irreversible changes had occurred in the monolayer after the first compression run: upon decompressing it eventually reaches an identical state as before compressing, even after it was compressed to beyond the transition point.

Molecular Weight Effects. Although in several publications it is argued that the molecular weight is not very important in determining the pressure–area isotherms of polymeric substances,[1,4,34] varying the molecular weight of the isotactic PMMA yields interesting results (Figure 5).

The most striking observation is the fact that, at 22 °C and compression speeds of 2 Å²/(monomeric unit min), with molecular weights less than about 20 000, the transition phenomenon in the pressure–area isotherm becomes less pronounced with decreasing molecular weight and eventually disappears; in the isotherms of samples 15 and 16 ($\bar{M}_n$ 4000 and 2800) no sign of the monolayer transition is detectable any longer, and the monolayer appears to remain in the expanded condition until it collapses. The fact that the isotacticity of the lowest molecular weight materials is somewhat less perfect than that of the higher molecular weight materials (Table I) cannot be held fully responsible for the complete disappearance of the transition features from the pressure–area isotherm of these lowest molecular weight fractions, since for higher molecular weight fractions of similar tacticities, this transition is still clearly observable. However, this decrease in tacticity will be an additional cause for the transition suppression observed using these samples. Above molecular weights of about 20 000 (up to 10^6), the pressure–area isotherms change very little with varying

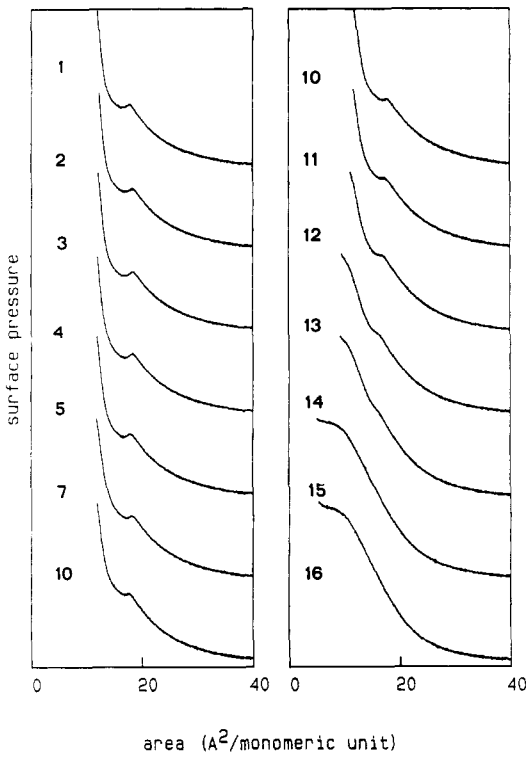

Figure 5. Pressure–area isotherms of isotactic PMMA of various molecular weights. Temperature 22 °C, compression speed 2 Å²/(monomeric unit min). Isotherms are cut off at 20 mN/m. The numbers in the figure correspond to Table I.

molecular weight. As far as the expanded phase is concerned, this is in agreement with theoretical predictions.[19]

The materials with "borderline" molecular weights (5000–15 000) have isotherms that are very sensitive to variations of temperature or compression rate. Using conditions that are more "critical" for the monolayer transition (higher temperatures, less perfect tacticities, high compression speeds), the critical molecular weight regime can be observed to extend to even higher molecular weights.

The Expanded Conformation. For an explanation of the different monolayer behavior of isotactic PMMA as compared to syndiotactic or atactic PMMA, we will first focus on the low-pressure part of the isotherms.

The thermodynamics of monolayers of polymeric substances have been described by several authors.[19,35,36] For the evaluation of the behavior of monolayers of steroregular PMMA we have chosen to use the equation of state theory as formulated by Matuura and Motomura.[19] They used a two-dimensional lattice model for polymeric monolayers similar to Singer's original approach,[35] but in their calculation of the equation of state they explicitly took into account both the entropic constraints of the limited available area as well as the enthalpic effects of the area-dependent number of intersegmental contacts on the lattice. Enthalpic effects due to cohesive lateral forces in the monolayer were not explicitly taken into account in Singer's original theory. Gabrielli and Huggins[36] later developed and used a more elaborate thermodynamic model of polymeric monolayers in which more parameters are used to describe physically relevant quantities. We have chosen to use the approach of Matuura and Motomura because of its simplicity and the low number of parameters that have to be fitted.

In the treatment of Maturra and Motomura the pressure of a monolayer of a polymeric substance is described in terms of the actual area per segment (A_0), the number of lattice sites available, the lattice coordination number Z, the number of segments per chain r, the temperature, and the enthalpy of contact between two neighboring segments on the lattice W.[19] In contrast to the "normal" convention for segment interaction parameters such as χ in the Flory–Huggins theory, a positive W value indicates a favorable enthalpic interaction (i.e., a negative interaction enthalpy). In contrast to Singer's theory the exact value of Z is not essential for a good fit to be obtained. In the examples Matuura and Motomura discussed, they used a coordination number of 4, which seems a realistic value for two-dimensional systems. In the treatment of Singer[35] very low Z values close to 2 are usually used (for condensed type monolayers), which do not seem to have a direct physically realistic meaning.[19] In the calculations we performed we used a standard value of 4 for the two-dimensional coordination number. With this value, the effect of the molecular weight is small as long as r does not get very small. In our fits of the isotherms we substituted the experimentally determined degree of polymerization $\bar{P}n$ for r. The area per monomeric unit A_0 and the interaction parameter W were varied so as to produce the best fit with the experimental data of the pressure–area isotherms. The absolute significance of the fit parameters is obviously subject to the limitations of the lattice model; e.g., possible pressure-induced changes in the lateral cohesive forces related to, e.g., a varying orientation of the segments are not accounted for, but in general this model proved to give satisfying results up to surface pressures of about 6 mN/m. The values obtained from the fit procedure are useful for relative comparisons.

In Figure 6a the pressure–area isotherm of isotactic PMMA, as calculated by the procedure described above, is drawn together with the experimental data (sample 5). It can be seen that the fit follows the experimental isotherm quite well up to a pressure of about 5 mN/m, approximately where the aforementioned "transition" starts to take place in the monolayer and begins to affect the experimentally determined isotherm. The fit parameters A_0 and W/kT can be varied only over a rather narrow range to produce acceptable fits: for the A_0 the fit uncertainty is only some tenths of Å²/monomeric unit, with an accompanying variation in the value for W/kT of several hundredths. The area per monomeric unit A_0 was not forced to be constant in fits of different isotherms, since this area can be imagined to vary with the surface conformation of the segments.

If we compare the values found for isotactic PMMA with those obtained from the fit of the isotherm of syndiotactic and atactic PMMA (Figure 6b,c), we see that the value for the intersegmental cohesion energy W is much higher for the latter materials (Table III). The value for A_0 is somewhat lower than that used for isotactic PMMA. The fact that the simulated curve for syndiotactic PMMA drops below zero pressure whereas the experimental curve does not is a consequence of the fact that the pressure is calculated for a "homogeneous" system, whereas in the real system phase separation can occur in the monolayer. The concentrated phase can be anticipated to have a specific area corresponding to the point where the calculated curve crosses the zero-pressure line, that is, where the free energy of the system has a minimum, $\Pi = \partial F/\partial A = 0$.[19]

We analyzed the isotherms of a series of PMMA samples of varying tacticities by this approach; the results are reported in Table III. The calculated lateral cohesive energy (W/kT) is plotted as a function of the diad tacticity in Figure 7. Starting from highly isotactic material, this value for W/kT increases rapidly as the meso diad content decreases.

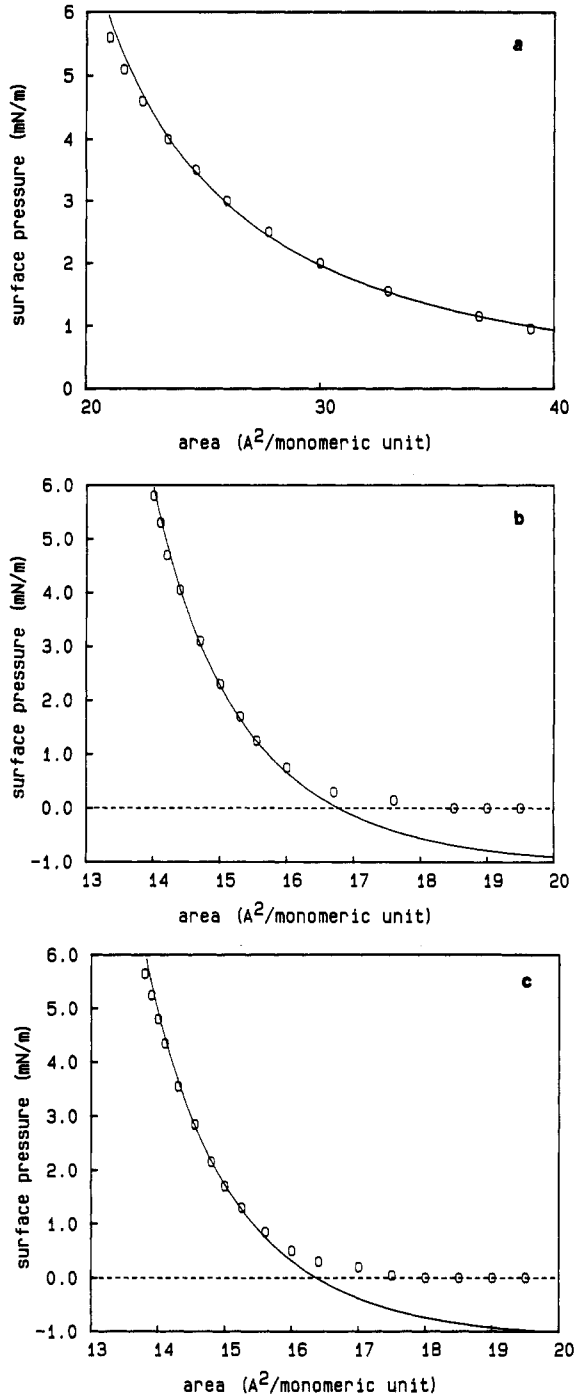

Figure 6. Pressure–area isotherms fitted by using the theory of Matuura and Motomura: (a) isotactic (sample 5); (b) "atactic" (sample 24); (c) syndiotactic (sample 25). Experimental data corresponding to isotherms at 22 °C, compression speed 3 Å²/(monomeric unit min).

Table III
Parameters Used To Fit Isotherms of PMMA Samples of Varying Tacticity (Temperature 22 °C)

sample	W/kT	A_0
5	0.29	13.7
17	0.37	13.6
18	0.43	13.2
21	0.62	13.0
24	1.35	12.2
25	1.38	12.1

To explain this apparently strong difference in cohesive energy, it is important to discuss the conformational characteristics of the isotactic and syndiotactic PMMA. Calculations on the various possible conformations of isotactic and syndiotactic PMMA have been carried out by

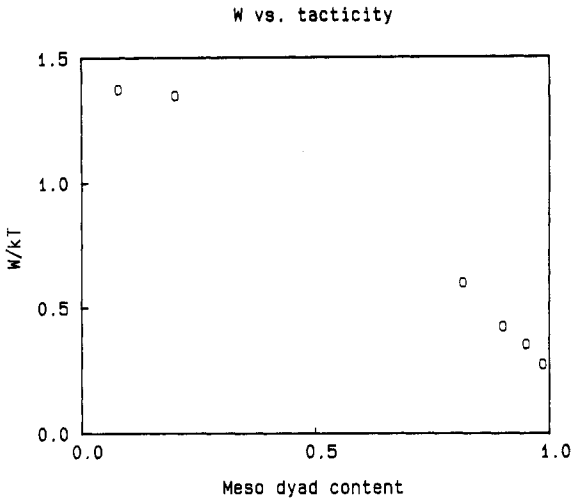

Figure 7. Values for W/kT used to obtain the best-fit experimental isotherms according to the theory of Matuura and Motomura, as a function of the meso diad content of the samples studied.

Vacatello and Flory[37] and by Sundarajan.[38,39] For isotactic PMMA the dominant backbone conformation corresponds to (slightly twisted) trans–trans orientations of successive C–C bonds, but other conformations will contribute significantly, since the energy differences are not very large: the backbone of isotactic PMMA is quite flexible. Syndiotactic PMMA has a much stronger preference for an all-trans backbone conformation; the energy of deviating backbone conformations is much higher, resulting in a very strong domination of all-trans backbone sequences. At the air–water interface, the energy of these macromolecules will of course strongly be affected by their asymmetric environment, but the intrinsic energy of the polymer itself (apart from its interaction with the interface) can be expected to provide extra boundary conditions for the conformational characteristics.

For isotactic PMMA, in this favorable nearly all-trans conformation, the ester groups are all more or less on the same side of the polymer. This would allow this part of the chain by a simple rotation to orient itself favorably with respect to an air–water interface like an amphiphilic molecule, with the hydrophilic part of the polymer (the ester groups) oriented toward the water phase and the hydrophobic part of the polymer (the hydrocarbon backbone with the α-methyl groups) on the air side. Furthermore, the flexibility of the isotactic PMMA backbone may easily allow small conformational adjustments, so as to optimize this amphiphilic orientation, which may well extend over a large number of segments. Such sequences of oriented segments can be argued to stabilize the orientation of the individual segments, since a segment cannot rotate completely independently from the neighboring segments, suggesting that some kind of cooperative effect may be operative in maintaining the amphiphilic segment orientation.

In contrast, for syndiotactic PMMA an alignment of its ester groups on the water side would require very strong deviations from the dominating all-trans backbone sequences, something that will be impeded by its low backbone flexibility. These suggested differences in ester group orientation of isotactic and syndiotactic PMMA may affect the lateral cohesive interactions between the segments. In isotactic PMMA the ester groups would tend to point downward toward the water phase, instead of more or less sideways in syndiotactic PMMA; the dipolar interactions between the ester groups would be screened by the water phase more effectively in the case of isotactic

Table IV
Values of W for Isotactic PMMA (Sample 5) Determined from Fits of Isotherms at Various Temperatures

temp, °C	$10^{-21}W$, J	temp, °C	$10^{-21}W$, J
10	0.7	32	1.8
22	1.2	41	2.4

PMMA, whereas in syndiotactic PMMA these dipolar interactions may contribute significantly stronger to the lateral cohesive forces in the monolayer.

The fact that for isotactic polymers the cohesive force increases very rapidly with increasing meso diad content may be explained by a cooperative effect as suggested above. The introduction of some defects (racemic diads) would locally affect the stabilization by such a cooperative effect and thus severely affect the overall orientational characteristics of the polymer. A comparison of the monolayer behavior of isotactic and syndiotactic poly(ethyl methacrylate) and poly(isobutyl methacrylate) yields similar conclusions as for PMMA: the monolayer behavior of the syndiotactic samples is characterized by larger values for W/kT, presumably through similar segmental orientational differences as discussed for poly(methyl methacrylate).

The unexpected temperature dependence of the surface pressure of the monolayer in the expanded condition (Figure 2) can also be explained by temperature-dependent lateral cohesive interaction energies. The order required to align the ester groups of the isotactic PMMA toward the water phase (and to minimize the lateral cohesive interactions) is likely to be disturbed by the thermal movements of the polymer chain segments as the temperature is raised; this is reflected in a higher value for W necessary to fit the experimental surface pressure data (Table IV).

The Transition in Isotactic PMMA. Information about the structural nature of the transition phenomenon can be obtained from grazing angle reflection infrared measurements on multilayers of isotactic PMMA transferred to a gold substrate. An extensive FT-IR study of the behavior of Langmuir–Blodgett films after transfer onto solid substrates is reported in the accompanying paper.[40] We will shortly discuss the main conclusions with respect to the nature of the monolayer transition here.

For thin films prepared by multiple transfer of the isotactic PMMA monolayers at low surface pressures (5 mN/m) onto a gold substrate, it is observed that the grazing angle reflection spectrum is practically identical with the spectrum that can be expected for a completely amorphous, randomly oriented thin film of isotactic PMMA. It was concluded that there were no indications that the multilayers, built by transfer at low surface pressures, deviates from a normal bulk structure in conformational and orientational characteristics, as far as this could be determined from the IR spectra. Apparently during transfer from the expanded condition the monolayer behaves as a collection of rather flexible polymer chains, the polymer being transferred in a more or less random conformation, in which no evidence of a deviating water surface orientation seems to be retained.

The grazing angle reflection spectrum of a thin film built of isotactic PMMA transferred at a surface pressure of 12 mN/m proved to be clearly different. In several absorption bands significant deviations can be found with respect to the amorphous, randomly oriented thin films.[40] All deviations could be matched with differences between the (bulk) transmission spectra of amorphous and crystalline isotactic PMMA. The IR results strongly indicate that at surface pressures beyond the transition pressure, the isotactic PMMA monolayer is transferred in a conformation that has definitely crystalline characteristics. The crystal structure of isotactic PMMA was studied by several authors and is now generally believed to be a 10/1 double helix,[41,42] so that it appears that double-helical structures of isotactic PMMA are formed at the water surface upon compression. For a more extensive discussion of the FT-IR results of the multilayers that all support this double-helix hypothesis, we refer to the accompanying paper.[40]

Calculating the area per monomeric unit that a 10/1 double helix of isotactic PMMA would occupy, on the basis of the crystal parameters reported in literature (helix diameter 12.5 Å, pitch 21.1 Å), yields a value of 13.2 Å^2/monomeric unit.[42] When we extrapolate the posttransition region (10–20 mN/m) of an isotherm that was recorded stepwise with the film being allowed to stabilize at each pressure to eliminate kinetic effects, we find, upon extrapolation to zero pressure, a specific area of 14.5 Å^2/monomeric unit, which approaches the calculated value for the double-helical structure. A deviation to the high area side of this extrapolated value can easily be caused by the presence of a small fraction of "amorphous" material with a high surface compressibility.

In the literature several polymers are reported that retain a helical conformation, formed in the spreading solvent, at the air–water interface,[43-46] but isotactic PMMA seems to be the first example of a polymer that acquires a stable helical structure induced by compression. As far as we know, no other synthetic materials assuming a double-helix structure at the air–water interface have been reported.

Although we have no absolute proof so far that the helix involved is the same as the double helix reported for the crystal structure, we think that the indications that it is are very strong. Another helical structure that was proposed for crystalline isotactic PMMA (a 5/1 single helix)[47] was dismissed later on, when the idea of the double helix was introduced. A helix such as that would occupy a significantly larger area per monomeric unit on the water surface, as compared to the values calculated for the 10/1 double helix and as compared to the experimentally determined values.

Returning to Figures 1–5 again, we can use the (double) helix formation hypothesis to explain the phenomena observed upon compression. At large areas the isotactic PMMA tends to form an expanded phase in which all segments are in contact with the water phase. This conformation would have a lower free energy than a helical structure of the chains, because of the higher monolayer entropy. When the monolayer is compressed, this entropy decreases. (The internal energy might also be affected at very small areas since it may get increasingly difficult for the monolayer to accommodate all segments in the most favorable conformation with respect to the interface.) When the entropy difference between the expanded phase and the helical phase becomes so small that it no longer compensates for possible differences in internal energy and the gain in free energy caused by the decrease of the occupied area upon transition to the helical structure (the $\Pi\Delta A$ contribution to the free energy of the transition), a transition takes place from the expanded conformation to the helical, pseudocrystalline phase. The temperature dependence of the isotherms (Figure 2) supports this suggestion: at higher temperatures the transition takes place at higher pressures, and if the temperature is too high, no such transition is detectable at all.

The monolayer transition does not take place instantaneously but requires time: this is reflected in the time dependence of the isotherms (Figure 3). The exact nature of the kinetic effects will be discussed later in this article.

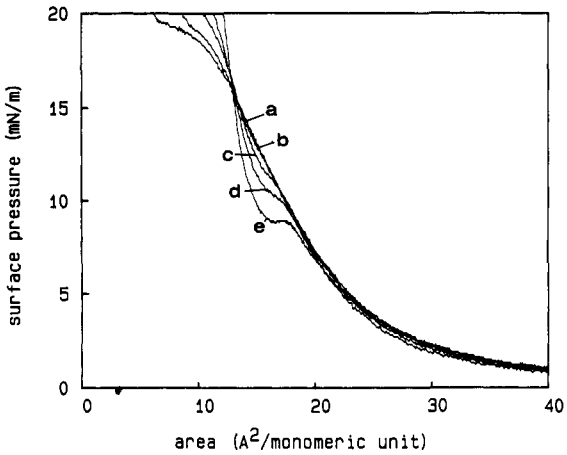

Figure 8. Pressure–area isotherm of mixtures of isotactic PMMA samples 5 ($\bar{M}_n$ 26 000) and 16 ($\bar{M}_n$ 2800). Temperature 22 °C, compression speed 12 Å²/(monomeric unit min). Weight fraction of the low molecular weight component: (a) 1.0, (b) 0.70, (c) 0.45, (d) 0.26, (e) 0.0.

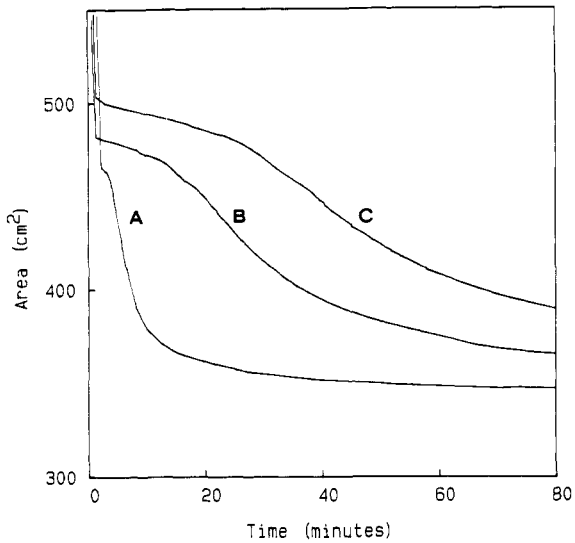

Figure 9. Stabilization experiments of isotactic PMMA (sample 5). Surface pressure: (A) 7.3, (B) 6.5, (C) 6.1 mN/m. Temperature 22 °C.

The remarkable molecular weight effect on the pressure–area isotherms can also be explained by using the helix hypothesis. For materials with low molecular weights the helix formation seems to become less favorable (Figure 5). The reason for this phenomenon may be found in the fact that the helix formation requires a *critical chain length*. Next to free energy contributions that are proportional to the number of segments involved (and thus to the length of the helix formed, through the internal energy and the $\Pi\Delta A$ contribution), a helix formation may also be expected to be associated with an initial entropy loss (e.g., the loss in translational entropy when two chains combine to form a double-helical structure) that would not depend directly on the length of the helix formed:

$$\Delta G_{helix} = -T\Delta S_{init} + N(\Delta U_{conform} - T\Delta S_{conform} + \Pi\Delta A_{conform})$$

where N is the number of monomeric segments in the helix.

The length of the helices will be determined by defects that may occur along the helix, e.g., by the presence of chain ends. Short chains will therefore be able to form only short helices (especially when a double helix is involved and end groups of both chains may disturb the helical sequence), and the free energy gain upon helix formation will consequently be lower. For the lowest molecular weight fractions, the second term might not be large enough to overcome an initial entropy loss. In bulk crystallization experiments we have found a similar suppression of the crystallization for the lowest molecular weight materials, presumably due to the same reasons. Critical chain length phenomena are well-known from studies of polymeric complexes and, e.g., template polymerizations.[48,49]

Molecular Weight Mixtures. The pressure–area isotherms of mixtures of isotactic PMMA of molecular weights 2800 and 36 000 (samples of 16 and 5) recorded at a compression rate of 12 Å²/(monomeric unit min) are shown in Figure 8. The molecular weights are chosen so as to have one component being able to form helices, the other component not being able to do so. We clearly see that the mixtures do not exhibit additive behavior: the amount of helix formation (to be estimated from the extent of departure from the isotherm associated with no monolayer transition) is obviously far too low compared to what can be expected on the basis of additive behavior, and the apparent onset pressure is too high. The helix formation process of the 36 000 molecular weight material is clearly affected by the presence of the low molecular weight material. The helix formation is not a locally isolated phenomenon, with parts of a chain independently being able to form felical structures, but instead involves (thermodynamically or kinetically) the environment of the individual helical structures to be formed.

Kinetic Effects. The fact that the pressure–area isotherm of isotactic PMMA shows a drop in pressure upon compression during the suggested helix formation seems puzzling at first sight. Apparently, when the helix formation starts to take place (at surface pressures just over 5 mN/m), the rate is slow and the area generated by the transition from the expanded conformation to the helical conformation cannot compensate for the decrease in area due to the compression, so that the surface pressure keeps rising, which causes the rate of helix formation to rise. When the area created per time unit by the transition equals the (constant) area consumed by the compression, the slope of the isotherm is zero: the "top" of the isotherm. After this point, the helix formation rate appears to increase even further, instead of remaining constant, leading to an actual increase of the area available for the non-helix phase and thus to a drop in the surface pressure. When the monolayer has been largely converted to the helix conformation, the absolute transition rate slows down naturally, and the pressure starts to rise again. If the increase in conversion rate would be only due to a rising pressure in the beginning of the process, it can be anticipated that the isotherm will bend to a zero slope, but this cannot explain why the pressure actually drops beyond this maximum, since this pressure drop would automatically slow down the helix formation rate resulting in a flat region where compression speed and transition rate are matched. In reality the helix formation rate must be autoaccelerating to produce the observed pressure dip.

We can explain these phenomena if we consider the helix formation as a two-dimensional crystallization process analogous to the three-dimensional crystallization process of isotactic PMMA. If we consider the helix formation as the result of an activated nucleation mechanism followed by a growth of the nuclei formed, an autoaccelerating effect can be anticipated.

To check this hypothesis, we performed stabilization experiments at surface pressures close to the transition pressures observed in the pressure–area isotherms for surface pressures of 6.1–7.3 mN/m, using sample 5. The results are shown in Figure 9. The area is directly

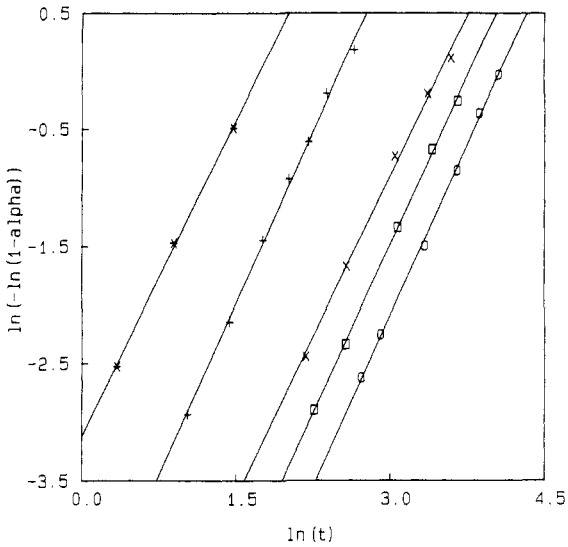

Figure 10. Results of Avrami analyses of stabilization experiments similar to Figure 14. Surface pressures: 6.1 (○), 6.3 (□), 6.5 mN/m (×), 6.8 (+), and 7.3 mN/m (*).

correlated to the amount of crystallization that has occurred in the monolayer. Remarkable is the S-shape of the curves representing the isobaric surface crystallization process, illustrating the autoaccelerating nature of the process.

Crystallization kinetics in three dimensions can be studied by using Avrami analyses. This approach can also be used for the two-dimensional crystallization process proposed here. Gabrielli[50] already reported using an Avrami type approach to describe the kinetics of collapse of PMMA monolayers at high surface pressures.

The well-known expression that Avrami proposed to describe the time dependence of the crystalline fraction during isothermal crystallization is[51]

$$1 - \alpha = \exp(-Kt^n)$$

where α is the mole fraction of crystalline material, K is a constant, t is time, and n is the Avrami exponent.

With isobaric and isothermal monolayer crystallization conditions (to ensure a constant molecular thermodynamic driving force), this equation may be expected to apply also to the helix formation process of isotactic PMMA at the water surface. The α can be estimated from the area lost referenced to the beginning of the crystallization divided by the area lost at the end of the process when the surface area becomes stable. The results of the Avrami analyses are shown in Figure 10. Crystallization at all pressures is characterized by parallel straight lines in the Avrami plot for all surface pressures studied, up to conversions of about 75%. The Avrami exponent calculated from the slope of these lines is found to be 1.8–2.0. This indicates that the two-dimensional crystallization of isotactic PMMA may be described either by a nonactivated nucleation followed by a two-dimensional growth or by an activated nucleation mechanism followed by a one-dimensional growth. This latter probability is the most likely when we consider the suggestion that helices are involved.

An isolated helix will lack stabilization due to lateral contacts with neighboring helices in the monolayer. During crystallization the helices will probably line up next to each other so as to optimize these lateral contacts, so that the free energy per helix is lowered. It is likely that there will be a critical nucleus size that renders the nucleus stable. Growth of the crystallite can then be expected mainly in the direction *perpendicular* to the helix

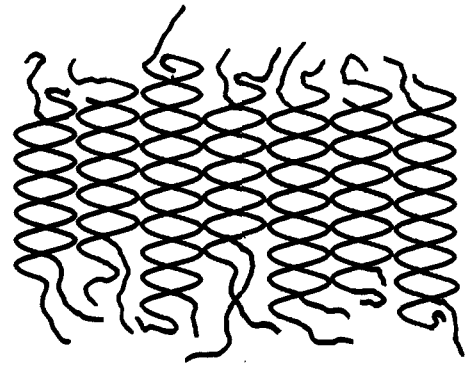

Figure 11. Schematic representation of a top view of the proposed water surface crystallites of isotactic PMMA.

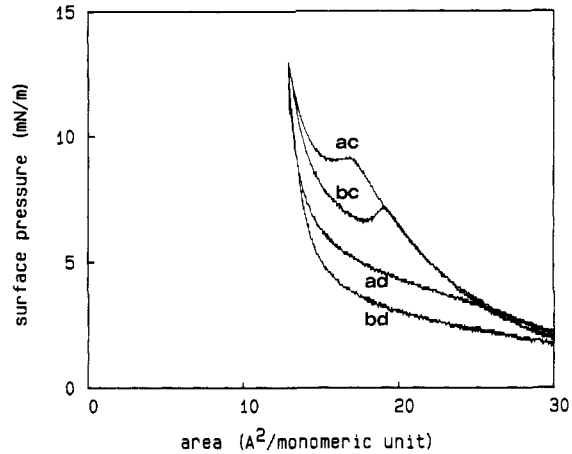

Figure 12. Hysteresis plots of isotactic PMMA (sample 5): (a) fast compression (10 Å²/(monomeric unit min)), pause time 0.5 min; (b) slow compression (0.2 Å²/(monomeric unit min)), pause time 30 min. Decompression speed in both cases was 10 Å²/(monomeric unit min). Compression curves are annotated with c, decompression curves with d.

direction. This is illustrated by Figure 11. This model is in agreement with the value found for the Avrami exponent and is also supported by the results reported in the accompanying paper.[40]

The crystallization kinetics depend on the molecular weight of the isotactic PMMA: lowering the molecular weight to the "critical" region results in severely suppressed crystallization rates at constant surface pressures. The surface pressure required to form stable nuclei is higher than for the 36 000 molecular weight material. The very strong dependence of the isotherms of borderline molecular weight PMMA on the compression speed is also a result of the suppressed nucleation: at high compression speeds the monolayer does not get the opportunity to produce enough nuclei to induce a reasonable overall crystallization rate, resulting in pressure–area isotherms in which the helix transition can hardly be observed.

Kinetic effects are also responsible for the difference in the hysteresis curves shown in Figure 12. The experiments differ in the speed of compression and the pause time at the maximum pressure. In both cases the monolayer "crystallization" has been completed to a large extent, the difference being that for the fast experiment a large number of small crystallites can be anticipated, whereas for the slow experiment (where the crystallization has taken place at lower pressures) a smaller number of larger crystallites can be expected. Upon decompresson (with equal decompression speeds) the monolayer that was rapidly crystallized clearly follows a "higher" path than the monolayer that was slowly crystallized. This may be due to the fact that larger crystallites are thermodynamically more stable and therefore decompose only at lower surface

pressures; the small crystallites of the fast experiment fall apart at higher pressures to assume an expanded configuration. The arguments of the crystallite size being important will also be encountered in the explanation of the lateral orientation effects during transfer.[40]

Conclusions

The behavior of monolayers of isotactic PMMA at the air–water interface is quite different from that of monolayers of syndiotactic PMMA. The fact that the isotactic polymer forms an expanded type monolayer whereas the syndiotactic polymer forms a condensed monolayer can be explained by the anticipated difference in lateral cohesive interactions. The transition that is observed at approximately 8 mN/m for a monolayer of isotactic PMMA upon compression can be explained by assuming that the isotactic PMMA is able to form double-helical structures at the water surface similar to those proposed for the bulk crystal structure. The formation of this double helix, suggested by infrared measurements, has not directly been proven yet, but a lot of circumstancial evidence indicates this possibility very strongly. Although helical conformations have been proposed for a number of polymers on the water surface, the fact that isotactic PMMA forms helices induced by compression has no analogue in monolayer literature; to our knowledge, no other examples of synthetic polymers existing as double helices at the air–water interface have been proposed so-far.

The monolayer behavior of isotactic PMMA is dependent on a series of parameters (molecular weight, tacticity, compression speed), so that the characteristics of the monolayer can be easily varied. This flexibility may make isotactic PMMA an interesting material for several applications. More results of the behavior of the Langmuir–Blodgett films after transfer to solid substrates, as studied by infrared techniques, are published in the accompanying paper.[40]

References and Notes

(1) Crisp, D. J. *J. Colloid Sci.* **1946**, *1*, 49.
(2) Crisp, D. J. *J. Colloid Sci.* **1946**, *1*, 161.
(3) Crisp, D. J. In *Surface phenomena in chemistry and biology*; Danielli, J. F., Pankhurst, K. G. A., Riddiford, A. C., Eds.; Pergamon Press: New York, 1958; p 23.
(4) Gaines, G. L., Jr. *Insoluble monolayers at liquid gas interfaces*; Interscience: New York, 1966.
(5) Mumby, S. J.; Swalen, J. D.; Rabolt, J. F. *Macromolecules* **1986**, *19*, 1054.
(6) Elbert, R.; Laschewsky, A.; Ringsdorf, H. *J. Am. Chem. Soc.* **1985**, *107*, 4134.
(7) Hong, K.; Rosner, R. B.; Rubner, M. F. *Chem. Mater.* **1990**, *2*, 82.
(8) Schneider, J.; Erdelen, C.; Ringsdorf, H.; Rabolt, J. F. *Macromolecules* **1989**, *22*, 3475.
(9) Nakahara, H.; Fukuda, K. *J. Colloid Interface Sci.* **1985**, *104*, 290.
(10) Lovelock, B. J.; Grieser, F.; Sanders, J. V. *J. Colloid Interface Sci.* **1985**, *108*, 297.
(11) Kawaguchi, M.; Sano, M.; Chen, Y.-L.; Zgrafi, G.; Yu, H. *Macromolecules* **1986**, *19*, 2606.
(12) Beredjick, N.; Ahlbeck, R. A.; Kwei, T. K.; Ries Jr., H. E. *J. Polym. Sci.* **1960**, *46*, 268.
(13) Beredjick, N.; Ries Jr., H. E. *J. Polym.* Sci. **1962**, *62*, 864.
(14) Hwa, J. C. H.; Ries Jr., H. E. *J. Polym. Sci., Polym. Lett.* **1964**, *2*, 389.
(15) Sutherland, J. E.; Miller, M. L. *J. Polym. Sci., Polym. Lett.* **1969**, *7*, 871.
(16) Kuan, S. W. J.; Frank, C. W.; Fu, C. C.; Allee, D. R.; Maccagno, P.; Pease, R. F. W. *J. Vac. Sci. Technol. B* **1988**, *6*(6), 2274.
(17) Stroeve, P.; Srinivasan, M. P.; Higgins, B. G.; Kowel, S. T. *Thin Solid Films* **1987**, *146*, 209.
(18) Sauer, B. B.; Yu, H.; Yazdanian, M.; Zografi, G.; Kim, M. W. *Macromolecules* **1989**, *22*, 2332.
(19) Motomura, K.; Matuura, R. *J. Colloid Sci.* **1963**, *18*, 52.
(20) Gabrielli, G.; Pugelli, M.; Baglioni, P. *J. Colloid Interface Sci.* **1982**, *86*, 485.
(21) Baglioni, P.; Dei, L.; Puggelli, M. *Colloid Polym. Sci.* **1985**, *283*, 266.
(22) Labbauf, A.; Zack, J. R. *J. Colloid Interface Sci*, **1971**, *35*, 569.
(23) Kowel, S. T.; Zhou, G.-G.; Srinivasan, M. P.; Stroeve, P.; Higgins, B. G. *Thin Solid Films* **1986**, *134*, 209.
(24) Kuan, S. W. J.; Frank, C. W.; Fu, C. C.; Allee, D. R.; Maccagno, P.; Pease, R. F. W. *J. Vac. Sci. Technol. B* **1988**, *6*, 2274.
(25) Kuan, S. W. J.; Martin, P. S.; Frank, C. W.; Pease, R. F. W. *Polym. Mater. Sci. Eng.* **1989**, *60*, 270.
(26) Kawaguchi, M.; Sauer, B. B.; Hyuk, Yu. *Macromolecules* **1989**, *22*, 1735.
(27) Dovek, M. M.; Albrecht, T. R.; Kuan, S. W. J.; Lang, C. A.; Emch, R.; Grütter, P.; Frank, C. W.; Pease, R. F. W.; Quate, C. F. *J. Microsc. (Oxford)* **1988**, *152*, 229.
(28) Albrecht, T. R.; Dovek, M. M.; Lang, C. A.; Grütter, P.; Quate, C. F.; Kuan, S. W. J.; Frank, C. W.; Pease, R. F. W. *J. Appl. Phys.* **1988**, *64*, 1178.
(29) Gabrielli, G.; Puggelli, M.; Faccioli, R. *J. Collid Interface Sci.* **1972**, *11*, 63.
(30) Gabrielli, G.; Puggelli, M.; Baglioni, P. *J. Colloid Interface Sci.* **1982**, *86*, 485.
(31) Goode, W. E.; Owens, F. H.; Feldmann, R. P.; Snijder, W. H.; Moore, J. H. *J. Polym. Sci.* **1960**, *46*, 317.
(32) Hatada, K.; Ute, K.; Tanaka, K.; Okamoto, Y.; Kitayama, T. *Polym. J.* **1986**, *18*, 1037.
(33) Abe, H.; Imai, K.; Matsumoto, M. *J. Polym. Sci. C* **1968**, *23*, 469.
(34) Llopis, J.; Subirana, J. A. *J. Colloid Sci.* **1961**, *16*, 618.
(35) Singer, S. J. *J. Chem. Phys.* **1948**, *16*, 872.
(36) Gabrielli, G.; Ferroni, E.; Huggins, M. L. *Prog. Colloid Polym. Sci.* **1975**, *58*, 201.
(37) Vacatello, M.; Flory, P. J. *Macromolecules* **1986**, *19*, 405.
(38) Sundarajan, P. R. *Macromolecules* **1986**, *19*, 415.
(39) Sundarajan, P. R. *Macromolecules* **1979**, *12*, 575.
(40) Brinkhuis, R. H. G.; Schouten, A. J. *Macromolecules*, following paper in this issue.
(41) Kusanagi, H.; Tadokoro, H.; Chatani, Y. *Macromolecules* **1976**, *9*, 531.
(42) Bosscher, F.; Ten Brinke, G.; Eshuis, A.; Challa, G. *Macromolecules* **1982**, *15*, 1364.
(43) Takeda, F.; Matsumoto, M.; Takenaka, T.; Fujiyoshi, Y.; Uyeda, N. *J. Colloid Interface Sci.* **1983**, *91*, 267 and references therein.
(44) Malcolm, B. R. *Polymer* **1966**, *7*, 595; *Prog. Surf. Membr. Sci.* **1973**, *7*, 183.
(45) Schoondorp, M. A.; Vorenkamp, E. J.; Schouten, A. J., submitted to *Thin Solid Films*.
(46) Loeb, G. I.; Baier, R. E. *J. Colloid Interface Sci.* **1968**, *27*, 38.
(47) Tadokoro, H.; Chatani, Y.; Kusanagi, H.; Yokoyama, M. *Macromolecules* **1970**, *3*, 441.
(48) Ten Brinke, G.; Schomaker, E.; Challa, G. *Macromolcules* **1985**, *18*, 1925.
(49) Schomaker, E.; Ten Brinke, G.; Challa, G. *Macromolecules* **1985**, *18*, 1930.
(50) Gabrielli, G.; Guarini, G. G. T. *J. Colloid Interface Sci.* **1978**, *64*, 185.
(51) Avrami, M. *J. Chem. Phys.* **1939**, *7*, 1103; **1940**, *8*, 212; **1941**, *9*, 177.

Registry No. i-PMMA, 25188-98-1; a-PMMA, 9011-14-7; s-PMMA, 25188-97-0.